Original Article *J. Clin. Biochem. Nutr.*, **46**, 212–223, May 2010

A Mouse Model of Metabolic Syndrome: Insulin Resistance, Fatty Liver and Non-Alcoholic Fatty Pancreas Disease (NAFPD) in C57BL/6 Mice Fed a High Fat Diet

Julio C. Fraulob, Rebeca Ogg-Diamantino, Caroline Fernandes-Santos, Marcia Barbosa Aguila and Carlos A. Mandarim-de-Lacerda*

Laboratory of Morphometry and Cardiovascular Morphology, Biomedical Center, Institute of Biology, State University of Rio de Janeiro, Av 28 de Setembro, 87 (fds) – CEP 20551-030, Rio de Janeiro, Brazil

Received 20 August, 2009; Accepted 23 December, 2009; Published online 10 April, 2010

Summary **Diet-induced obesity in C57BL/6 mice triggers common features of human metabolic syndrome (MetS). The purpose is to assess the suitability of a diet-induced obesity model for investigating non-alcoholic fatty pancreatic disease (NAFPD), fatty liver and insulin resistance. Adult C57BL/6 mice were fed either high-fat chow (HFC, 60% fat) or standard chow (SC, 10% fat) during a 16-week period. We evaluated in both groups: hepatopancreatic injuries, pancreatic islets size, alpha and beta-cell immunodensities, intraperitoneal insulin tolerance test (IPITT) and oral glucose tolerance test (OGTT). The HFC mice displayed greater mass gain ($p<0.0001$) and total visceral fat pads ($p<0.001$). OGTT showed impairment of glucose clearance in HFC mice ($p<0.0001$). IPITT revealed insulin resistance in HFC mice ($p<0.0001$). The HFC mice showed larger pancreatic islet size and significantly greater alpha and beta-cell immunodensities than SC mice. Pancreas and liver from HFC were heavier and contained higher fat concentration. In conclusion, C57BL/6 mice fed a high-fat diet develop features of NAFPD. Insulin resistance and ectopic accumulation of hepatic fat are well known to occur in MetS. Additionally, the importance of fat accumulation in the pancreas has been recently highlighted. Therefore, this model could help to elucidate target organ alterations associated with metabolic syndrome.**

Key Words: **metabolic syndrome, insulin resistance, fatty liver, non-alcoholic fatty pancreatic disease, high-fat diet**

Introduction

Obesity leads to the infiltration of fat in multiple organs including the heart, kidneys, liver, and pancreas. When accompanied by insulin resistance or type 2 diabetes (T2D), hypertension and dyslipidemia significantly increase the risk for cardiovascular disease [*1*]; in patients suffering from metabolic syndrome (MetS), this risk is even greater [*2*].

High-fat diet (HFD) is a nutritional condition that accounts for the largest incidence of MetS in the world [*3*]. A major cause of steatosis, also known as fatty liver disease, is increased fatty acid flux to the liver, which is promoted by a high availability of plasma free fatty acids (FFAs) in relation to peripheral oxidative requirements. Several conditions increase fatty acid flux to the liver, pancreas and adipose tissue [*4–6*]. Consequently, elevated insulin levels generate oxidative stress and organ injuries [*5*, *7*]. The pathophysiological consequence of fat infiltration is an increase in cellular FFAs and decreased beta-oxidation, ultimately resulting in triglyceride accumulation. This accumulation manifests as an increase in dietary FFAs and lipolysis in peripheral fat tissue [*4*, *8*].

In general, there is continuous cycling and redistribution

*To whom correspondence should be addressed.
Tel: (+55.21) 2587-6416 Fax: (+55.21) 2587-6133
E-mail: mandarim@uerj.br

of non-oxidized fatty acids between different organs. An early event in the development of obesity is an increase in visceral adipose tissue, particularly in the size of the white adipocytes. This transformation is seen to precede the development of fatty liver and insulin resistance, which are marked on a cellular level by hepatic fat infiltration and tumor necrosis factor alpha (TNF-alpha) expression [*6*].

Infiltration of the liver by fat, or nonalcoholic fatty liver disease (NAFLD), is a major form of chronic liver disease in adults and children. NAFLD is one consequence of the current obesity epidemic, and can progress to nonalcoholic steatohepatitis (NASH), which is characterized by steatosis, inflammation, and progressive fibrosis, ultimately leading to cirrhosis and end-stage liver disease [*9*, *10*]. Likewise, infiltration of the pancreas by fat or NAFPD, is characterized by a heavier pancreas due to more pancreatic fat, consisting of a high composition of triglycerides and FFAs, as well as increased cytokine production [*5*, *11*]. Pancreatic fat accumulation can compromise normal pancreatic function. Under conditions of oxidative stress, fat-derived cytokines are released locally and may result in inflammatory processes associated with organ dysfunction. In addition, elevated levels of circulating FFAs alone are implicated in beta-cell dysfunction, leading to increased basal insulin release and impaired glucose-stimulated insulin secretion by beta-cells [*12–14*].

In T2D, beta-cells eventually fail to meet the demand created by insulin resistance, leading to hyperglycemia. However, in most of these disorders, the beta-cells compensate for the insulin resistance for long periods with an increase in secretory capacity, an increase in beta-cell mass, or both. However, the factors that contribute to beta-cell hyperplasia in insulin resistant states remain poorly understood [*12*].

In the present study, we sought to evaluate structural adaptations in pancreas, liver and fat storage in response to an increased dietary supply of fat using a C57BL/6 mouse model of high-fat diet-induced insulin resistance, a model that displays several correlations to human MetS.

Materials and Methods

Animals and diets

Eight-week-old male C57BL/6 mice were used in this study, housed in a temperature-controlled (21 ± 2°C) room on a 12:12 h dark-light cycle with free access to food and water. All procedures were carried out in accordance with conventional guidelines for experimentation with animals (NIH Publication Nº. 85-23, revised in 1996) and experimental protocols were approved by the local Committee.

Mice were separated into two groups ($n = 10$ for each group) and fed different diets during a 16 week period: high-fat chow (HFC, 26% of calories from carbohydrates, 60% from fat, and 14% from protein), or standard chow (SC, 76% of calories from carbohydrates, 10% from fat, and 14% from protein). The mineral and vitamin content of the two diets were identical and in accordance with the American Institute of Nutrition's recommendation (AIN 93M) [*15*] (details in Table 1). Fresh chow was provided daily and any chow remaining from the previous day was discarded. Food intake was evaluated daily (1 p.m.), and body mass was measured weekly. Caloric content of food intake was determined based on 5.404 kcal/g for high-fat and 3.573 kcal/g for standard chow diets. The feed efficiency (FE) [(weight gained/kcal consumed) × 100] was determined after 16 weeks on the respective diets.

Table 1. Composition and energy content of the standard chow (SC) and high-fat chow (HFC).

Content (g/Kg)	Diets	
	SC	HFC
Casein (≥85% de protein)	140	190
Cornstarch	620.7	250.7
Sucrose	100	100
Soybean oil	40	40
Lard	—	320
Fiber	50	50
Vitamin mix*	10	10
Mineral mix*	35	35
L-Cystin	1.8	1.8
Choline	2.5	2.5
Antioxidant	0.008	0.008
Total grams	1,000	1,000
Energy content (Kcal/Kg)	3,573	5,404
Carbohydrates (%)	76	26
Protein (%)	14	14
Lipids (%)	10	60

*Mineral and vitamin mixtures.

Oral glucose tolerance test (OGTT)

Fasting blood glucose was measured (6 h fast, blood taken from the tail vein) according to manufacturers' recommendations using an Accu-Chek glucometer (Roche Diagnostics GmbH, Mannheim, Germany). Glucose was then administrated by gavage (25% glucose solution, 1 g/kg mice) and blood glucose was measured again at time points of 15, 30, 60 and 120 min, post gavage.

Intraperitoneal Insulin tolerance test (IPITT)

Fasting blood glucose was measured (4 h fast, blood taken from the tail vein) using a glucosimeter (Roche Diagnostics GmbH, Mannheim, Germany). Insulin was then injected intraperitoneally (1 U/kg) and blood glucose was measured again at time points of 15, 30, 60 and 120 min, post injection.

Euthanasia

After 16 weeks on a diet, mice were deeply anesthetized (intraperitoneal sodium pentobarbital, 45 mg/kg) and blood samples were rapidly obtained by cardiac puncture of the right atrium. Plasma was then obtained by centrifugation (120 g for 15 min) at room temperature and stored individually at −20°C until biochemical analyses were performed.

Pancreas, liver and fat pads (epididymal, retroperitoneal and perirenal fat pads) were carefully removed and weighed. Organ masses were then analyzed relative to tibia length in order to standardize body biometry (we used the left tibia length for this standardization because body masses varied within the groups; the left tibia was dissected and the distance between the condyle to the tip of the medial malleolus was measured) [*16*]. Tissue was then rapidly fixed in freshly prepared fixative solution (formaldehyde 4% w/v, 0.1 M phosphate buffer, pH 7.2) for analysis by light microscopy.

Biochemical analysis

Total cholesterol and triglycerides (TG) were assayed by the colorimetric enzymatic method. The high-density lipoprotein-cholesterol (HDL-c) was measured using the kinetic-colorimetric method, according to the manufacturer's instructions (Bioclin System II, Quibasa, Belo Horizonte, MG, Brazil). The low-density lipoprotein-cholesterol (LDL-c) was obtained via the Friedwald's formula [*17*, *18*]. The enzymes alanine aminotransferase (ALT), aspartate aminotransferase (AST) and alkaline phosphatase (ALK) were also measured.

Radioimmunoassay for insulin and costicosterone and HOMA-IR

Plasma insulin concentrations were measured using an insulin RIA (radioimmunoassay) kit (Linco Research, St. Charles, MO, Cat. RI-13K) and plasma corticosterone concentrations were measured using a corticosterone RIA kit (Immuchem Double Antibody, MP Biomedicals, Orangeburg, NY). All samples were analyzed in a double assay format, for which the intra-assay coefficient of variation was 1.4% for insulin and 4.4% for corticosterone. The HOMA-IR (homeostasis model assessment of insulin resistance) index was calculated as [fasting serum glucose × fasting serum insulin/22.5] to assess insulin resistance [*17*].

Liver, pancreas and adipose tissue

Small pieces of liver, pancreas and epididymal fat pads were embedded in Paraplast plus (Sigma-Aldrich, St. Louis, MO), sectioned at 5 μm and then stained with hematoxylin-eosin. The liver sections were observed under light microscopy (Olympus BX51 microscope), in order to investigate the structure of the hepatic lobule and hepatocyte steatosis.

The pancreatic islet is nearly circular, allowing for determination of the mean islet diameter based on the greatest and smallest diameters in the equatorial islet plane. These measurements were made with the software Image-Pro Plus version 5.0 (Media Cybernetics, Silver Spring, MD) with a sample size of at least 200 islets per group (digital images TIFF format, 36-bit color, 1280 × 1024 pixels, LC Evolution camera and Olympus BX51 microscope).

The pancreas islet number was estimated with the physical disector-fractionator method (for details see [*19–21*]). Briefly, in a consecutive series of sections, starting with a random section, for example number 10, and leaving an interval of 50 sections, we determined the primary sections (sections numbers 60, 110, 160 etc.). From the intervals between these primary sections, we separated the reference sections (e.g. section numbers 18, 68, 118, 168, and so on) used to quantify the total number of pancreatic islet by the physical fractionator method. The distance between primary and reference sections was 40 μm for each step. This represents about 1/4 of the islet diameter in this animal. Thus, islets seen at primary sections (e.g. section 10) but not in the reference sections (e.g. section 18) were counted. The remaining sections were used for immunohistochemical analysis and observation of interlobular and intralobular fat deposits.

To estimate the cross-sectional area of adipocytes, at least 50 adipocytes per animal were measured with the software Image-Pro Plus version 5.0 (Media Cybernetics—digital images TIFF format, 36-bit color, 1280 × 1024 pixels, LC Evolution camera and Olympus BX51 microscope).

Immunohistochemistry

Antigen retrieval was performed using citrate buffer pH 6.0, and endogenous peroxidase was quenched by hydrogen peroxide 3%. Sections were then incubated with rabbit anti-glucagon (A0565, Dako) and guinea pig anti-insulin (A0564, Dako) antibodies for 2 h. Subsequently, samples were treated with a biotinylated secondary antibody (K0679, Universal DakoCytomation LSAB + Kit, Peroxidase, Glostrup, Denmark), which was detected by reaction with horseradish peroxidase-streptavidin-biotin complex. Positive immunoreactions were identified following incubation with 3,3' diaminobenzidine tetrachloride (K3466, DAB, DakoCytomation) and sections were then counterstained with Mayer hematoxylin.

Digital images of the stained slices were obtained (LC Evolution camera, Olympus BX51 microscope, TIFF format, 36-bit color, 1280 × 1024 pixels) and analyzed with the software Image-Pro Plus version 5.0 (Media Cybernetics). The density threshold selection tool was used to select the areas of the pancreatic islet marked with insulin and glucagon, which was then expressed as a percentage of the islet mean cross-sectional area (immuno-density). The average of 10 islets per animal was calculated for each group.

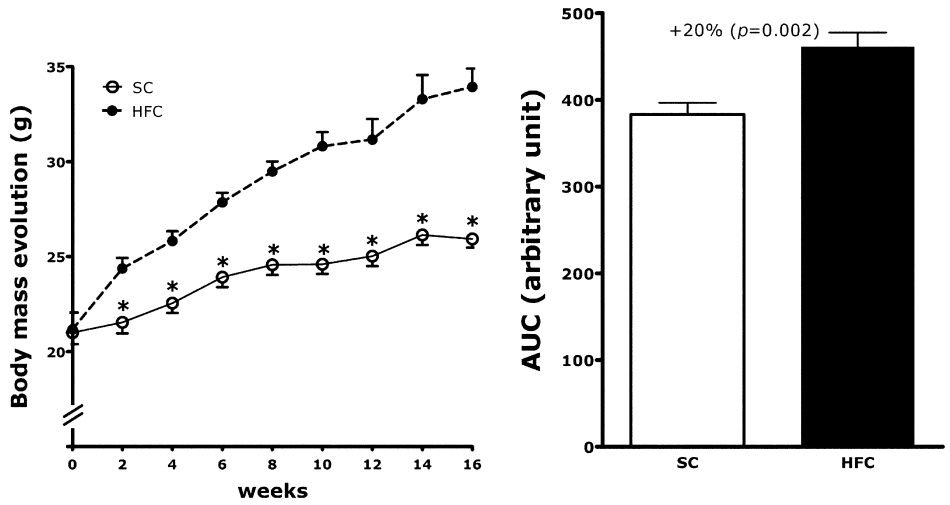

Fig. 1. Body mass. Body mass evolution and respective areas under the curve (AUC) show significant differences between the body mass gain in the standard chow (SC) group and in the very high-fat chow (HFC) group. Values are mean ± SEM, n = 10/group. *p<0.05, different from HFC Group.

Table 2. Body composition, food and fat intakes and feed efficiency in mice fed standard chow (SC) and high-fat chow (HFC).

Biometry and Nourishment data	Groups		SC vs HFC
	SC	HFC	p
Final body weight, g	25.9 ± 0.4	33.9 ± 0.7	<0.001
Body weight gain, g/week	0.3 ± 0.09	0.7 ± 0.1	0.01
Pancreas/Tibial, g/cm	0.11 ± 0.01	0.13 ± 0.01	0.03
Liver/Tibial, g/cm	0.44 ± 0.01	0.56 ± 0.01	<0.001
Total visceral fat	1.1 ± 0.4	2.7 ± 0.4	<0.001
Food intake, g/day/mice	2.4 ± 0.06	2.2 ± 0.1	ns
Energy intake, Kcal/day/mice	8.4 ± 0.2	11.9 ± 0.1	<0.001
Lipid intake, Kcal/day/mice	0.8 ± 0.02	7.1 ± 0.2	<0.001
Feed efficiency, %	0.5 ± 0.1	0.9 ± 0.1	0.01

Values are mean ± SEM (n = 8/group). Data were analyzed by Student's t test.

Data analysis

The data are displayed as mean and standard error of the mean (SEM). Differences between the groups were analyzed with the Student t test and a p value ≤0.05 was considered as statistically significant (GraphPad Prism 5.1, GraphPad Software, La Jolla, CA).

Results

Body mass, fat pads and adipocyte morphometry

HFC mice had greater mass gain compared to SC mice (Fig. 1, Table 2). Significant body mass differences were observed from the second week. At the 16th week, body mass was more than 30% greater in HFC mice than in SC (p = 0.002). Likewise, the fat pads were significantly larger in HFC mice than in SC mice: total visceral fat pads (+143%, p = 0.003), retroperitoneal fat (+124%, p<0.01), epididymal fat (+90%, p<0.01) (Fig. 2). The morphometry of adipocytes showed adipocyte hypertrophy in HFC mice when compared to SC mice (adipocyte diameter varied from 56.7 ± 0.5 μm in SC mice to 86.5 ± 0.9 μm in HFC mice, +52%, p<0.0001) (Fig. 2).

Food intake and feed efficiency

Food intake was not different between the groups, but both the energy (+38%, p<0.05) and fat intake per animal (+729%, p<0.001) were greater in HFC mice than in SC (Table 2). Feed efficiency (body mass gain in grams per kilocalories consumed) was therefore greater in HFC mice than in SC mice (Fig. 3).

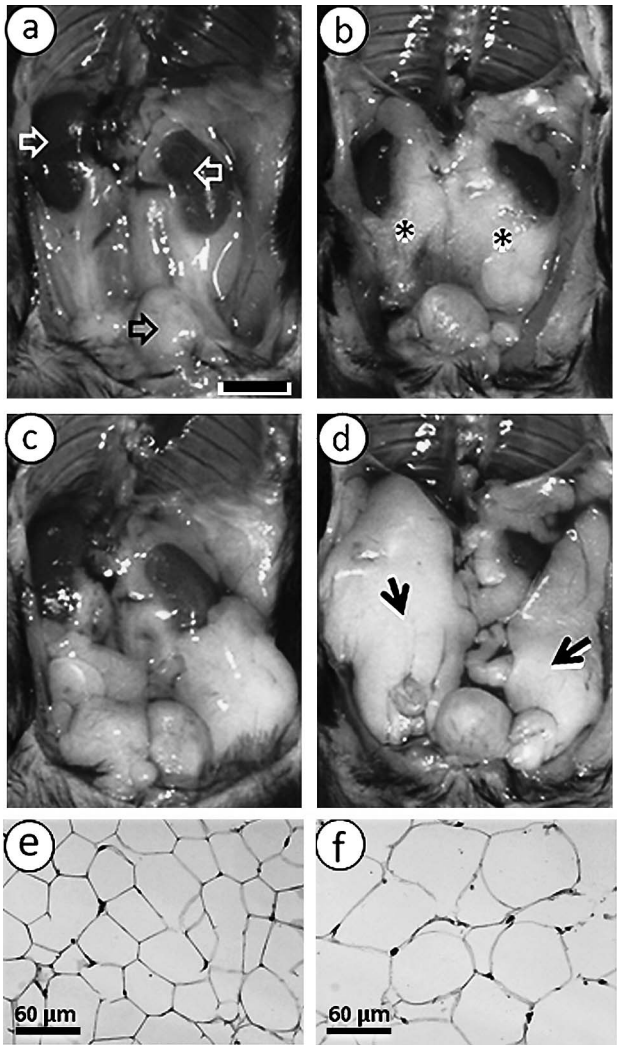

Fig. 2. Fat pads. Abdominal ventral view of dissected mice showing the fat pads (bar = 2.5 mm): Retroperitoneal fat pads: (a) SC group, the kidneys (white open arrows) are surrounded by small fat pads extending until the urinary bladder (black open arrow); (b) HFC group, the fat pads (asterisks) are greater than in SC group, covering partially the kidneys. Epididymal fat pads: (c) SC group—they cover up the inferior abdominal cavity but are much more developed in HFC group (d) (arrows). Photomicrographs of adipocytes (hematoxylin and eosin stain—bar = 60 µm). (e) shows typical epididymal fat adipocytes from lean mice fed SC and (f) shows adipocytes for the HFC group, with greater diameter.

Blood biochemistry

Plasma levels of TG ($p = 0.001$), HDL-c ($p = 0.002$) and LDL-c ($p = 0.02$), but not total cholesterol, were higher in HFC mice than in SC mice. Plasma ALT ($p = 0.01$), AST ($p<0.001$) and ALK ($p<0.001$) concentrations were also significantly elevated in the HFC mice when compared to SC mice (Table 3).

Homeostasis model assessment of insulin resistance and plasma costicosterone

Both the fasting plasma glucose ($p = 0.01$) and insulin ($p = 0.02$) were increased in HFC mice in comparison with SC mice. Therefore, HFC mice presented higher HOMA-IR ($p<0.001$) and higher levels of plasma costicosterone than SC mice (Table 3).

OGTT and IPITT

In the OGTT, the plasma glucose increased to a maximum after 15 min of oral administration of glucose in both groups, but this maximum was higher in HFC mice than in SC mice ($p<0.0001$). The time-course of glucose clearance in HFC mice was delayed compared to SC mice, remaining elevated for 120 min ($p<0.001$) after glucose administration, qualifying for characterization as glucose intolerance (Fig. 4).

The IPITT demonstrated a quick decline in plasma glucose after 15 min of insulin administration in both groups, but plasma glucose remained higher in HFC mice than in SC mice ($p<0.0001$) at all time-points up to 120 min (Fig. 5), characterizing the HFC mice as insulin resistant.

Structure of liver and pancreas

Liver was heavier (+25%, $p = 0.03$) and showed macro- and microvesicular steatosis in HFD fed mice. Pancreas was also heavier (+19%, $p = 0.03$) and had greater ectopic fat deposition within pancreatic tissue, characterized by intralobular and interlobular fatty deposition in HFC mice compared to SC mice (Fig. 6).

The HFC mice showed larger pancreatic islets (islet diameter varied from 115.2 ± 4.2 µm in SC mice to 151.3 ± 5.3 µm in HFC mice, +30%, $p<0.01$), and significantly greater alpha and beta-cell immune-densities than SC mice (Fig. 7, 8). As usual, positive immunostaining for glucagon (alpha-cells) was found primarily at the islet periphery (Fig. 7), while immunostaining for insulin (beta-cells) was found primarily at the islet central zone (Fig. 8).

Discussion

This study demonstrates that adult C57BL/6 mice fed a high-fat diet (60% fat) developed glucose intolerance, insulin resistance and hepatopancreatic structural alterations characterized by macro- and micro-steatosis, islet hypertrophy and increased alpha and beta-cell immune-densities, beyond that expected from simply having increased body biometry and fat storage. We also observed dyslipidemia and expected high HDL-c levels in C57BL/6 mice [*22*], with altered high plasma levels of ALT, AST and ALK. Plasma glucose, insulin and costicosterone were also enhanced by HFD administration, characterizing insulin resistance in the animals.

Pancreatic ectopic fat accumulation in the interlobular

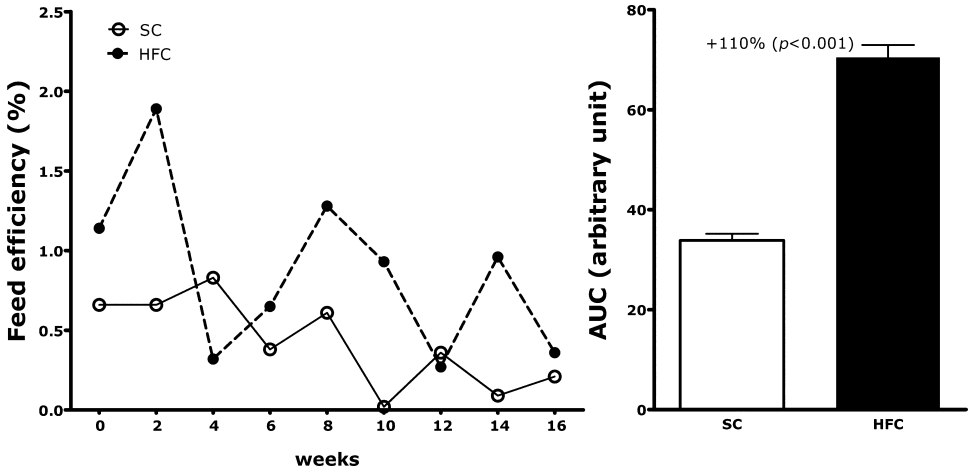

Fig. 3. Feed efficiency. Feed efficiency (values are means) measured in standard chow (SC) group and in very high-fat chow (HFC) group. The areas under the curve (AUC) show the differences between the groups. Values are mean ± SEM, $n = 10$/group.

Table 3. Blood biochemistry

Parameter	Groups		SC vs HFC
	SC	HFC	*p*
Glucose, mmol/L	8.3 ± 0.3	9.8 ± 0.4	0.01
Insulin, pmol/L	120.8 ± 1.1	219.8 ± 38.7	0.02
HOMA-IR index[1]	44.6 ± 5.3	95.7 ± 10.2	<0.001
Costicosterone (ng/mL)	68.7 ± 14.0	148.4 ± 30.6	0.03
Cholesterol, mg/dl	95.7 ± 3.5	104.0 ± 4.3	ns
LDL-c, mg/dl	41.8 ± 3.5	54.0 ± 2.5	0.02
HDL-c, mg/dl	54.0 ± 1.5	63.0 ± 2.2	0.002
Triglycerides, mg/dl	23.9 ± 2.6	43.9 ± 4.0	<0.001
AST, UI/l	245.2 ± 16.2	321.4 ± 6.2	<0.001
ALP, UI/l	47.4 ± 5.2	67.4 ± 4.6	0.01
ALK, UI/l	37.5 ± 5.7	76.0 ± 6.2	<0.001

[1]fasting insulin concentration (pmol/L) × fasting glucose concentration (mmol/L)/22.5
Values are mean ± SEM; n of 5–7 mice/group. LDL-c, low-density lipoprotein-cholesterol; HDL-c, high-density lipoprotein-cholesterol; AST, aspartate aminotransferase; ALK, alkaline phosphatase; ALT, alanine aminotransferase; SC, standard chow; HFC, high-fat chow.

space (around the great vessels and ducts) and in the intralobular space (within the exocrine pancreas) was observed after chronic HFD intake, suggesting NAFPD, which may result in chronic pancreatitis. This observation is important because experimental evidence supports the notion that high-fat intake can induce hyperlipidemia and lead to pancreatic endocrine and exocrine alterations [*23*], with increased pancreatic FFA, lipid peroxidation and collagen synthesis by activated pancreatic stellate cells [*24*], and histopathological alterations resulting from an acute inflammatory response in the early stages of secondary pancreatic acinar cell atrophy and fibrosis [*11*, *25*].

Fatty acid intake displays time-dependent and deposit-specific effects in mice [*26*]. In addition, it impairs the regulation of pancreatic beta-cell cAMP production, a signaling pathway important for adequate islet adaptation to a perturbed metabolic environment. Normally this process is protective against the development of glucose intolerance and insulin resistance [*12*, *27*]. C57BL/6 mice responded to oversupply of dietary fat with adipose tissue remodeling, through adipocyte hyperplasia and hypertrophy in agreement with a previous report [*28*]. This is an important issue because adipose tissue expresses various secretory proteins, including leptin, TNF-alpha and adiponectin, which may be involved in the regulation of energy expenditure, lipid metabolism and insulin resistance [*29*].

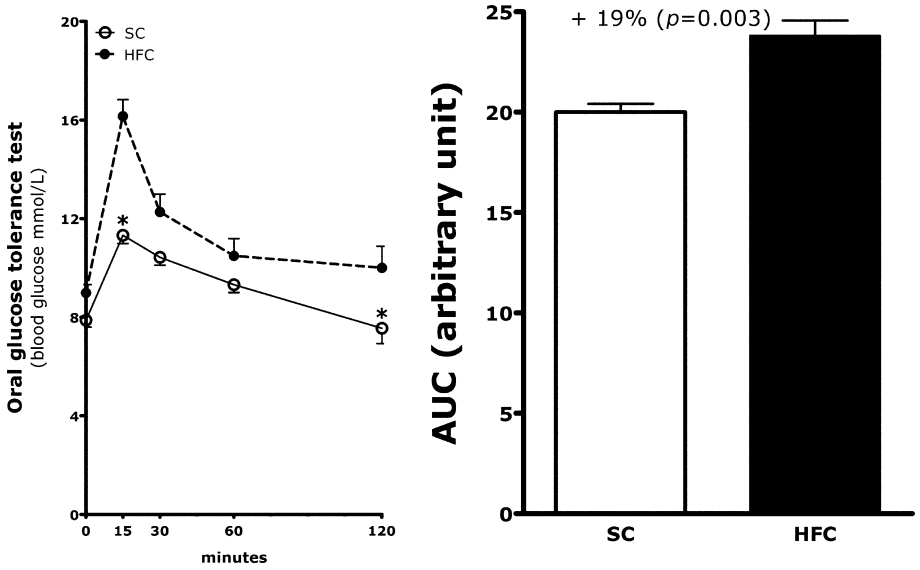

Fig. 4. Oral glucose tolerance test. Oral glucose tolerance test curve at 14th week. The areas under the curve show significant differences between the standard chow (SC) group and the very high-fat chow (HFC) group. Values are mean ± SEM, n = 5/group. *p<0.05, different from HFC Group.

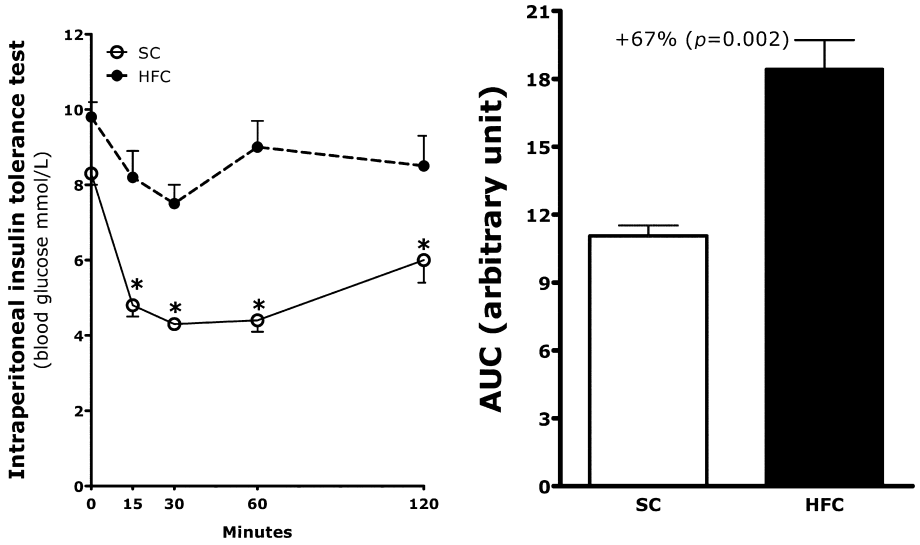

Fig. 5. Intraperitoneal insulin tolerance test. Intraperitoneal insulin tolerance test curve at 15th week. The areas under the curve show significant differences between the standard chow (SC) group and the very high-fat chow (HFC) group. Values are mean ± SEM, n = 5/group. *p<0.05, different from HFC Group.

Plasma adiponectin levels decrease during obesity, and are negatively associated with plasma insulin, positively associated with plasma triglycerides, and correlate with increases in HOMA-IR [*6*]. Low levels of adiponectin decrease fatty acid oxidation in the muscle, and this effect is mediated by the interaction with muscle and hepatic receptors through activation of AMP kinase, the cellular "fuel gauge", which, in turn, inhibits acetyl CoA carboxylase and increases fatty acid beta-oxidation [*30*]. Additionally, decreased adiponectin levels have been implicated in the development of steatosis in mouse models of obesity and lipodystrophy [*31*].

The HOMA-IR index is associated with myocardial ischemia, independent of established risk factors [*32*]. Severe insulin resistance may impair glucose-stimulated insulin secretion, thereby undermining beta-cell compensation and leading to hyperglycemia. Moreover, because insulin stores are intact, the secretory defects reflect an

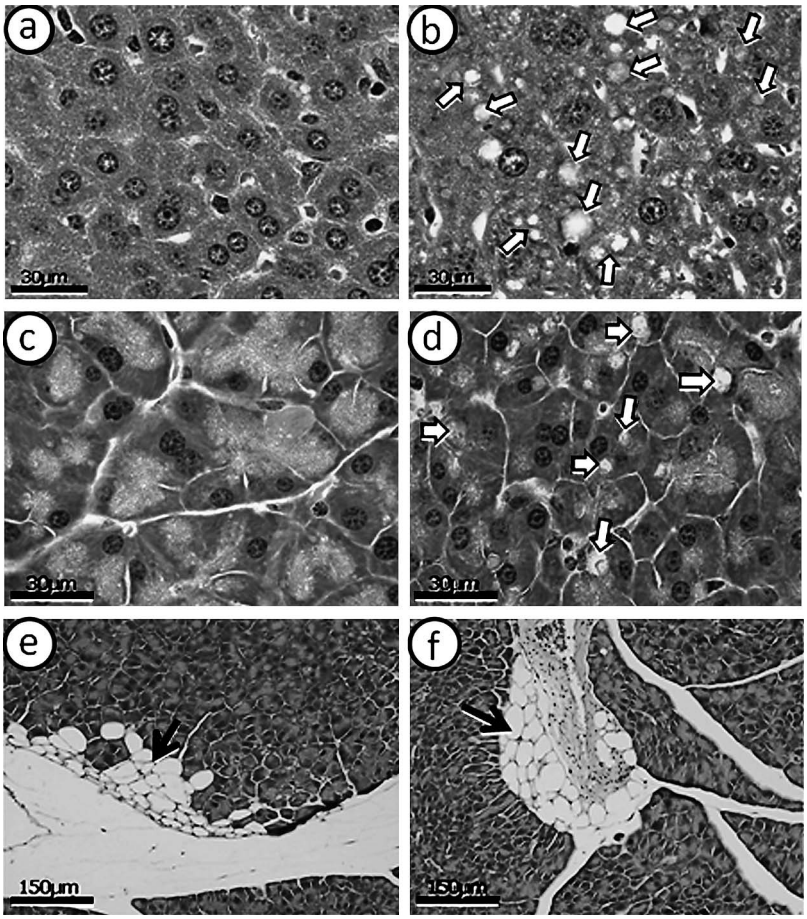

Fig. 6. Photomicrographs of liver and pancreas. Photomicrographs of liver and pancreas (hematoxylin and eosin stain): (a) typical liver of a lean mice fed SC and (b) liver of high-fat fed mice with macro- and microvesicular steatosis (arrows); (c) typical pancreas of a lean mice fed SC and (d) pancreas of high-fat fed mice showing intracellular lipid vesicles in acinar cells (arrows); (e) adipose infiltration in pancreas of high-fat fed mice (black arrow) and (f) ectopic deposition of the interlobular fat of high-fat fed mice (black arrow).

early stage of beta-cell dysfunction [*33*]. The mice fed HFD clearly displayed an elevated HOMA-IR index that is compatible with the presence of insulin resistance in these animals. One mechanism by which dietary overload of lipids appears to lead to the development of insulin resistance and T2D in C57BL/6J mice is by an increased saturation of phospholipids of the mitochondrial membrane, leading to decreased mitochondrial function [*34*]. In addition, the failure of islet beta-cells to compensate for impaired insulin-stimulated glucose disposal is one of the main mechanisms underlying the onset of hyperglycemia and overt T2D [*35*].

The fatty liver is insulin resistant [*36*]. Liver fat is highly and linearly correlated with all components of the MetS, independent of obesity [*2*]. Therefore, NAFLD is emerging as component of the MetS [*9*, *37*]. NAFLD markers ALT and AST predict MetS independently of potential confounding variables [*38*]. Serum ALT elevations have been used as a surrogate biomarker for NAFLD and steatohepatitis in the clinical setting. ALT activity is normally present at low levels in the circulation of standard chow fed mice. In high fat/cholesterol fed mice, the incidence and severity of elevated plasma ALT levels increased significantly as a function of the time the animals were maintained on this diet [*22*, *39*]. Clinical evidence demonstrates that fatty pancreas is associated with higher levels for visceral fat, AST, ALT, total cholesterol, triglyceride, insulin, and the HOMA-IR [*40*]. Likewise, C57BL/6 mice fed a HFD showed elevated ALT, AST and ALK plasma concentrations indicating alteration of the hepatic and pancreatic function.

Chronic stress is associated with derangement of metabolic homeostasis, a process that contributes to the clinical presentation of visceral obesity, T2D, atherosclerosis and MetS. Obesity constitutes a chronic stressful state that may cause hypothalamic-pituitary-adrenal (HPA) axis dysfunction [*41*]. Basal HPA axis activity and expression of its central regulatory markers are age-dependent in mice [*42*].

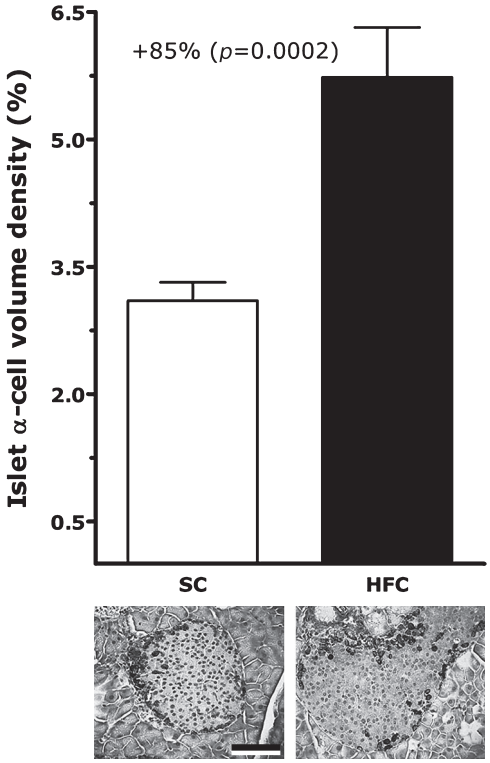

Fig. 7. Pancreatic islet alpha-cell. The pancreatic islet alpha-cell volume densities in the standard chow (SC) group and in the very high-fat chow (HFC) group were measured by image analysis. It was significantly greater in the HFC group. Photomicrographs under de column bars show typical islets of the two groups with positive stain for glucagon (same magnification, bar = 40 μm). Values are mean ± SEM, n = 10/group.

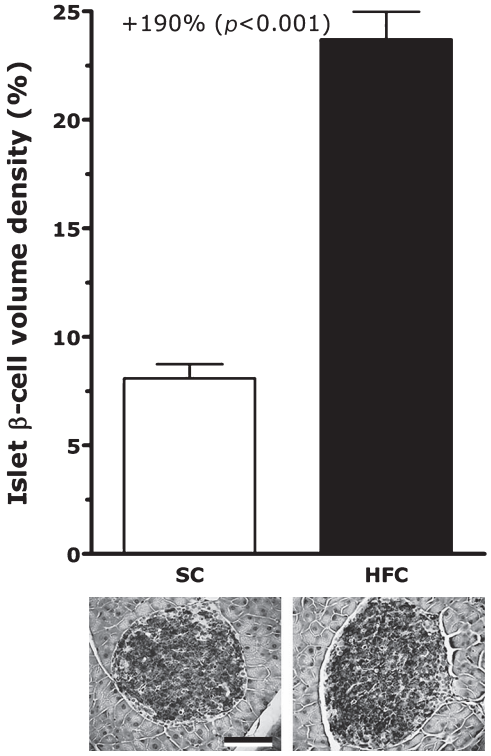

Fig. 8. Pancreatic islet beta-cell. The pancreatic islet beta-cell volume densities in the standard chow (SC) group and in the very high-fat chow (HFC) group were measured by image analysis. It was significantly greater in the HFC group. Photomicrographs under de column bars show typical islets of the two groups with positive stain for insulin (same magnification, bar = 40 μm). Values are mean ± SEM, n = 10/group.

Furthermore, dietary fat intake acts as a background form of chronic stress, elevating basal corticosterone levels and enhancing HPA response to stress [*43*]. The combination of stress and MetS increases the risk of cardiovascular disease [*1*]. In the present study, in spite of having carefully controlled for effects of age, mice fed HFD had significantly higher levels of plasma costicosterone than control mice. This corticosterone index could be correlated with an increase in both obesity and symptoms of metabolic syndrome [*43*].

By feeding mice a HFD, this study has arrived at several striking observations. In addition to observing the development of insulin resistance in mice fed a chronic HFD, we observed structural alterations such as liver macro and micro steatosis, larger pancreatic islets, greater alpha and beta-cell immuno-densities and ectopic fat deposition within pancreatic tissue. These observations seem to be alterations due to oversupply of lipids and are independent of the aging process in mice. Increased islet size and pancreatic insulin content in old non-obese (21–25-month-old) C57BL/6J male mice have already been reported [*44*]. A nearly twofold increase in islet size was correlated with a twofold increase of glucose-stimulated insulin secretion from perifused islets from 25-month-old males compared with 5-month-old males. Thus, the findings that glucose tolerance did not deteriorate with age, coupled with the lack of evidence for impaired beta-cell responsiveness to glucose in old males, suggest that the deterioration in glucose homeostasis seen in this study is not an inevitable consequence of aging in mice.

We found greater alpha and beta-cell immuno densities in mice fed HFD, but no differences in the islet distribution of these cells. Adeghate and co-workers found a similar percentage of insulin-positive (around 80%) and glucagon-positive cells (around 10%) in C57BL/6 mice fed fat-enriched diet compared to mice fed control diet [*45*]. It is also possible to demonstrate this effect by analyzing the density of immunolabeled cells, as measured by image analysis. By examining this in both groups, significant variations in densities of both cell types were found.

Insulin and glucagon are all secreted from the endocrine

pancreas, and both participate in the regulation of energy homeostasis. Increased expression of glucagon in the islets is proportionally related to an increase of its concentration in the blood [*46–47*]. By using a differential energetic base in age matched animals fed a diet higher in fat and carbohydrates (C57BL/6 mice fed a high-fat-high-sucrose diet, consisting of 44% carbohydrates with 16% sucrose and 42% fat), had increased pancreatic insulin and lower glucagon content [*11*, *13*]. Thus, pancreatic glucagon content appears to be influenced by food composition [*48*].

The liver is also simultaneously influenced by competing signals with regard to glucose secretion, since glucagon both stimulates insulin secretion and increases hepatic glucose output. Glucagon acts mainly in the liver, where it increases glucose production, while generating signals to reduce energy intake. Insulin acts directly at the liver to suppress the synthesis and secretion of glucose, and some plasma insulin is transported into the brain where it provides an important and indeed necessary input for the appropriate regulation of both stored energy and glucose secretion by the liver [*49*]. This analysis is important because the pancreatic beta-cell function is regulated by insulin signaling pathways. Insulin receptor substrate 2-dependent signaling in pancreatic islets is required not only for the maintenance of normal alpha and beta-cell mass, but is also involved in the regulation of insulin secretion [*50*, *51*].

Currently, many studies have reported that C57BL/6 mice develop obesity, insulin resistant, diabetes mellitus, hypertriglyceridemia [*11*, *13*] and advanced fatty liver disease when fed a high-fat diet, mimicking human metabolic syndrome. Compared with other animal models, such as Zucker obese rats, ob/ob or db/db mice or other gene deletion animal models, these HFD mice more closely resemble human obesity, serving as a model of exogenous obesity, which arises via a higher dietary caloric intake (fat overload) [*52*].

We now report, using stereological methods, that the pancreas of high-fat fed mice develops intracellular lipid vesicles in acinar cells, adipose infiltration and ectopic deposition of the interlobular fat, in addition to macro- and microvesicular steatosis in liver.

The HFD mouse model may promote a better experimental system in which to investigate MetS, by providing a model to examine interventions that prevent progression of fatty liver and fatty pancreas disease and to correlate the degree of liver and pancreatic steatosis with metabolic syndrome.

In conclusion, C57BL/6 mice fed a high fat diet develop features of both non-alcoholic fatty liver disease and non-alcoholic fatty pancreatic disease, a condition that is closely related to MetS. Ectopic accumulation of fat in liver and pancreas is a well-known symptom of MetS. However, only recently has the importance of fat accumulation in these tissues been highlighted. Therefore, the HFD animal model could help us to better understand the target organ alterations associated with metabolic syndrome and engender the possibility of developing novel treatments.

Acknowledgments

This work was supported by the agencies CNPq (Brazilian Council of Science and Technology, www.cnpq.br) and FAPERJ (Rio de Janeiro State Foundation for Scientific Research, www.faperj.br).

The authors are grateful to Mrs. Thatiany Marinho and Leonardo Mendonça for their technical assistance.

Abbreviations

AIN93, American Institute of Nutrition's recommendation; ALK, alkaline phosphatase; ALT, alanine aminotransferase; AST, aspartate aminotransferase; T2D, type 2 diabetes; FE, feed efficiency; FFAs, free fatty acids; TNF-alpha, tumor necrosis factor alpha; HDL-c, high-density lipoprotein-cholesterol; HFC, high fat chow; HOMA-IR, homeostasis model assessment-insulin resistance; LDL-c, low-density lipoprotein-cholesterol; IPITT, intraperitoneal insulin tolerance test; MetS, metabolic syndrome; NAFLD, nonalcoholic fatty liver disease; NAFPD, nonalcoholic fatty pancreas disease; NASH, nonalcoholic steatohepatitis; OGTT, oral glucose tolerance test; SC, standard chow; SEM, standard error of the mean; TG, triglycerides.

References

[1] Bonora, E.: The metabolic syndrome and cardiovascular disease. *Ann. Med.*, **38**, 64–80, 2006.

[2] Kotronen, A. and Yki-Jarvinen, H.: Fatty liver: a novel component of the metabolic syndrome. *Arterioscler. Thromb. Vasc. Biol.*, **28**, 27–38, 2008.

[3] Buettner, R., Scholmerich, J., and Bollheimer, L.C.: High-fat diets: modeling the metabolic disorders of human obesity in rodents. *Obesity (Silver Spring)*, **15**, 798–808, 2007.

[4] den Boer, M., Voshol, P.J., Kuipers, F., Havekes, L.M., and Romijn, J.A.: Hepatic steatosis: a mediator of the metabolic syndrome. Lessons from animal models. *Arterioscler. Thromb. Vasc. Biol.*, **24**, 644–649, 2004.

[5] Mathur, A., Marine, M., Lu, D., Swartz-Basile, D.A., Saxena, R., Zyromski, N.J., and Pitt, H.A.: Nonalcoholic fatty pancreas disease. *HPB (Oxford)*, **9**, 312–318, 2007.

[6] Akagiri, S., Naito, Y., Ichikawa, H., Mizushima, K., Takagi, T., Handa, O., Kokura, S., and Yoshikawa, T.: A mouse model of metabolic syndrome; increase in visceral adipose tissue precedes the development of fatty liver and insulin resistance in high-fat diet-fed male KK/Ta mice. *J. Clin. Biochem. Nutr.*, **42**, 150–157, 2008.

[7] Chitturi, S., Abeygunasekera, S., Farrell, G.C., Holmes-

Walker, J., Hui, J.M., Fung, C., Karim, R., Lin, R., Samarasinghe, D., Liddle, C., Weltman, M., and George, J.: NASH and insulin resistance: Insulin hypersecretion and specific association with the insulin resistance syndrome. *Hepatology*, **35**, 373–379, 2002.

[8] Pessayre, D.: Role of mitochondria in non-alcoholic fatty liver disease. *J. Gastroenterol. Hepatol.*, **22** Suppl. 1, S20–27, 2007.

[9] Jiang, J. and Torok, N.: Nonalcoholic steatohepatitis and the metabolic syndrome. *Metab. Syndr. Relat. Disord.*, **6**, 1–7, 2008.

[10] Gentile, C.L. and Pagliassotti, M.J.: The role of fatty acids in the development and progression of nonalcoholic fatty liver disease. *J. Nutr. Biochem.*, **19**, 567–576, 2008.

[11] Fernandes-Santos, C., Evangelista Carneiro, R., Mendonca, L.S., Aguila, M.B., and Mandarim-de-Lacerda, C.A.: Rosiglitazone aggravates nonalcoholic Fatty pancreatic disease in C57BL/6 mice fed high-fat and high-sucrose diet. *Pancreas*, **38**, e80–86, 2009.

[12] Yoshikawa, H., Tajiri, Y., Sako, Y., Hashimoto, T., Umeda, F., and Nawata, H.: Effects of free fatty acids on beta-cell functions: a possible involvement of peroxisome proliferator-activated receptors alpha or pancreatic/duodenal homeobox. *Metabolism*, **50**, 613–618, 2001.

[13] Nascimento, F.A., Barbosa-da-Silva, S., Fernandes-Santos, C., Mandarim-de-Lacerda, C.A., and Aguila, M.B.: Adipose tissue, liver and pancreas structural alterations in C57BL/6 mice fed high-fat-high-sucrose diet supplemented with fish oil (n-3 fatty acid rich oil). *Exp. Toxicol. Pathol.*, **62**, 17–25, 2010.

[14] Lee, Y., Hirose, H., Ohneda, M., Johnson, J.H., McGarry, J.D., and Unger, R.H.: Beta-cell lipotoxicity in the pathogenesis of non-insulin-dependent diabetes mellitus of obese rats: impairment in adipocyte-beta-cell relationships. *Proc. Natl. Acad. Sci. U.S.A.*, **91**, 10878–10882, 1994.

[15] Reeves, P.G., Nielsen, F.H., and Fahey, G.C. Jr.: AIN-93 purified diets for laboratory rodents: final report of the American Institute of Nutrition ad hoc writing committee on the reformulation of the AIN-76A rodent diet. *J. Nutr.*, **123**, 1939–1951, 1993.

[16] Yin, F.C., Spurgeon, H.A., Rakusan, K., Weisfeldt, M.L., and Lakatta, E.G.: Use of tibial length to quantify cardiac hypertrophy: application in the aging rat. *Am. J. Physiol.*, **243**, H941–947, 1982.

[17] Friedewald, W.T., Levy, R.I., and Fredrickson, D.S.: Estimation of the concentration of low-density lipoprotein cholesterol in plasma, without use of the preparative ultracentrifuge. *Clin. Chem.*, **18**, 499–502, 1972.

[18] Fukuyama, N., Homma, K., Wakana, N., Kudo, K., Suyama, A., Ohazama, H., Tsuji, C., Ishiwata, K., Eguchi, Y., Nakazawa, H., and Tanaka, E.: Validation of the Friedewald equation for evaluation of plasma LDL-cholesterol. *J. Clin. Biochem. Nutr.*, **43**, 1–5, 2008.

[19] Vogeser, M., Konig, D., Frey, I., Predel, H.G., Parhofer, K.G., and Berg, A.: Fasting serum insulin and the homeostasis model of insulin resistance (HOMA-IR) in the monitoring of lifestyle interventions in obese persons. *Clin. Biochem.*, **40**, 964–968, 2007.

[20] Bock, T., Pakkenberg, B., and Buschard, K.: Genetic background determines the size and structure of the endocrine pancreas. *Diabetes*, **54**, 133–137, 2005.

[21] Mandarim-de-Lacerda, C.A.: Stereological tools in biomedical research. *An. Acad. Bras. Cienc.*, **75**, 469–486, 2003.

[22] Zheng, S., Hoos, L., Cook, J., Tetzloff, G., Davis, H. Jr., van Heek, M., and Hwa, J.J.: Ezetimibe improves high fat and cholesterol diet-induced non-alcoholic fatty liver disease in mice. *Eur. J. Pharmacol.*, **584**, 118–124, 2008.

[23] Chowdhury, P., Nishikawa, M., Blevins, G.W. Jr., and Rayford, P.L.: Response of rat exocrine pancreas to high-fat and high-carbohydrate diets. *Proc. Soc. Exp. Biol. Med.*, **223**, 310–315, 2000.

[24] Zhang, X., Cui, Y., Fang, L., and Li, F.: Chronic high-fat diets induce oxide injuries and fibrogenesis of pancreatic cells in rats. *Pancreas*, **37**, e31–38, 2008.

[25] Yan, M.X., Li, Y.Q., Meng, M., Ren, H.B., and Kou, Y.: Long-term high-fat diet induces pancreatic injuries via pancreatic microcirculatory disturbances and oxidative stress in rats with hyperlipidemia. *Biochem. Biophys. Res. Commun.*, **347**, 192–199, 2006.

[26] Bueno, A.A., Oyama, L.M., de Oliveira, C., Pisani, L.P., Ribeiro, E.B., Silveira, V.L., and Oller do Nascimento, C.M.: Effects of different fatty acids and dietary lipids on adiponectin gene expression in 3T3-L1 cells and C57BL/6J mice adipose tissue. *Pflugers Arch.*, **455**, 701–709, 2008.

[27] Walz, H.A., Harndahl, L., Wierup, N., Zmuda-Trzebiatowska, E., Svennelid, F., Manganiello, V.C., Ploug, T., Sundler, F., Degerman, E., Ahren, B., and Holst, L.S.: Early and rapid development of insulin resistance, islet dysfunction and glucose intolerance after high-fat feeding in mice overexpressing phosphodiesterase 3B. *J. Endocrinol.*, **189**, 629–641, 2006.

[28] Strissel, K.J., Stancheva, Z., Miyoshi, H., Perfield, J.W. 2nd., Jick, Z., Greenberg, A.S., and Obin, M.S.: Adipocyte death, adipose tissue remodeling, and obesity complications. *Diabetes*, **56**, 2910–2918, 2007.

[29] Ahima, R.S.: Adipose tissue as an endocrine organ. *Obesity (Silver Spring)*, **14** Suppl 5, 242S–249S, 2006.

[30] Gil-Campos, M., Canete, R.R., and Gil, A.: Adiponectin, the missing link in insulin resistance and obesity. *Clin. Nutr.*, **23**, 963–974, 2004.

[31] Yamauchi, T., Kamon, J., Waki, H., Terauchi, Y., Kubota, N., Hara, K., Mori, Y., Ide, T., Murakami, K., Tsuboyama-Kasaoka, N., Ezaki, O., Akanuma, Y., Gavrilova, O., Vinson, C., Reitman, M.L., Kagechika, H., Shudo, K., Yoda, M., Nakano, Y., Tobe, K., Nagai, R., Kimura, S., Tomita, M., Froguel, P., and Kadowaki, T.: The fat-derived hormone adiponectin reverses insulin resistance associated with both lipoatrophy and obesity. *Nat. Med.*, **7**, 941–946, 2001.

[32] Gazzaruso, C., Solerte, S.B., De Amici, E., Mancini, M., Pujia, A., Fratino, P., Giustina, A., and Garzaniti, A.: Association of the metabolic syndrome and insulin resistance with silent myocardial ischemia in patients with type 2 diabetes mellitus. *The American journal of cardiology*, **97**, 236–239, 2006.

[33] Asghar, Z., Yau, D., Chan, F., Leroith, D., Chan, C.B., and Wheeler, M.B.: Insulin resistance causes increased beta-cell mass but defective glucose-stimulated insulin secretion in a murine model of type 2 diabetes. *Diabetologia*, **49**, 90–99, 2006.

[34] de Wilde, J., Mohren, R., van den Berg, S., Boekschoten, M., Dijk, K.W., de Groot, P., Muller, M., Mariman, E., and Smit, E.: Short-term high fat-feeding results in morphological and metabolic adaptations in the skeletal muscle of C57BL/6J mice. *Physiol. Genomics*, **32**, 360–369, 2008.

[35] Ahren, B. and Pacini, G.: Islet adaptation to insulin resistance: mechanisms and implications for intervention. *Diabetes Obes. Metab.*, **7**, 2–8, 2005.

[36] Lautamaki, R., Borra, R., Iozzo, P., Komu, M., Lehtimaki, T., Salmi, M., Jalkanen, S., Airaksinen, K.E., Knuuti, J., Parkkola, R., and Nuutila, P.: Liver steatosis coexists with myocardial insulin resistance and coronary dysfunction in patients with type 2 diabetes. *Am. J. Physiol. Endocrinol. Metab.*, **291**, E282–290, 2006.

[37] Machado, M. and Cortez-Pinto, H.: Non-alcoholic steatohepatitis and metabolic syndrome. *Curr. Opin. Clin. Nutr. Metab. Care*, **9**, 637–642, 2006.

[38] Hanley, A.J., Williams, K., Festa, A., Wagenknecht, L.E., D'Agostino, R.B. Jr., and Haffner, S.M.: Liver markers and development of the metabolic syndrome: the insulin resistance atherosclerosis study. *Diabetes*, **54**, 3140–3147, 2005.

[39] Tipoe, G.L., Ho, C.T., Liong, E.C., Leung, T.M., Lau, T.Y., Fung, M.L., and Nanji, A.A.: Voluntary oral feeding of rats not requiring a very high fat diet is a clinically relevant animal model of non-alcoholic fatty liver disease (NAFLD). *Histol. Histopathol.*, **24**, 1161–1169, 2009.

[40] Lee, J.S., Kim, S.H., Jun, D.W., Han, J.H., Jang, E.C., Park, J.Y., Son, B.K., Jo, Y.J., Park, Y.S., and Kim, Y.S.: Clinical implications of fatty pancreas: correlations between fatty pancreas and metabolic syndrome. *World J. Gastroenterol.*, **15**, 1869–1875, 2009.

[41] Kyrou, I. and Tsigos, C.: Stress mechanisms and metabolic complications. *Horm. Metab. Res.*, **39**, 430–438, 2007.

[42] Dalm, S., Enthoven, L., Meijer, O.C., van der Mark, M.H., Karssen, A.M., de Kloet, E.R., and Oitzl, M.S.: Age-related changes in hypothalamic-pituitary-adrenal axis activity of male C57BL/6J mice. *Neuroendocrinology*, **81**, 372–380, 2005.

[43] Tannenbaum, B.M., Brindley, D.N., Tannenbaum, G.S., Dallman, M.F., McArthur, M.D., and Meaney, M.J.: High-fat feeding alters both basal and stress-induced hypothalamic-pituitary-adrenal activity in the rat. *Am. J. Physiol.*, **273**, E1168–1177, 1997.

[44] Leiter, E.H., Premdas, F., Harrison, D.E., and Lipson, L.G.: Aging and glucose homeostasis in C57BL/6J male mice. *Faseb J.*, **2**, 2807–2811, 1988.

[45] Adeghate, E., Christopher Howarth, F., Rashed, H., Saeed, T., and Gbewonyo, A.: The effect of a fat-enriched diet on the pattern of distribution of pancreatic islet cells in the C57BL/6J mice. *Ann. N.Y. Acad. Sci.*, **1084**, 361–370, 2006.

[46] Ferrannini, E., Muscelli, E., Natali, A., Gabriel, R., Mitrakou, A., Flyvbjerg, A., Golay, A., and Hojlund, K.: Association of fasting glucagon and proinsulin concentrations with insulin resistance. *Diabetologia*, **50**, 2342–2347, 2007.

[47] Winzell, M.S., Brand, C.L., Wierup, N., Sidelmann, U.G., Sundler, F., Nishimura, E., and Ahren, B.: Glucagon receptor antagonism improves islet function in mice with insulin resistance induced by a high-fat diet. *Diabetologia*, **50**, 1453–1462, 2007.

[48] Bonnevie-Nielsen, V.: Different effects of high glucose and high fat diet on pancreatic insulin and glucagon in female and male mice. *Diabete Metab.*, **8**, 271–277, 1982.

[49] Woods, S.C., Lutz, T.A., Geary, N., and Langhans, W.: Pancreatic signals controlling food intake; insulin, glucagon and amylin. *Philos. Trans. R. Soc. Lond. B. Biol. Sci.*, **361**, 1219–1235, 2006.

[50] Cantley, J., Choudhury, A.I., Asare-Anane, H., Selman, C., Lingard, S., Heffron, H., Herrera, P., Persaud, S.J., and Withers, D.J.: Pancreatic deletion of insulin receptor substrate 2 reduces beta and alpha cell mass and impairs glucose homeostasis in mice. *Diabetologia*, **50**, 1248–1256, 2007.

[51] Weir, G.C. and Bonner-Weir, S.: A dominant role for glucose in beta-cell compensation of insulin resistance. *J. Clin. Invest.*, **117**, 81–83, 2007.

[52] Gallou-Kabani, C., Vige, A., Gross, M.S., Rabes, J.P., Boileau, C., Larue-Achagiotis, C., Tome, D., Jais, J.P., and Junien, C.: C57BL/6J and A/J mice fed a high-fat diet delineate components of metabolic syndrome. *Obesity (Silver Spring)*, **15**, 1996–2005, 2007.